Project 2 Report for Autonomous Space Robotics (ROB-GY 7863, CSCI-GA 3033 7863), Fall 2025

Denis Mbey Akola and Raman Kumar Jha

I. Introduction

Terrain Relative Navigation (TRN) is an autonomous navigation approach that enables vehicles, such as spacecraft and rovers, to estimate their position and orientation by analyzing the surrounding terrain. In the absence of GPS and under challenging visual conditions such as harsh illumination, deep shadows, and low-texture regions,traditional navigation methods are often unreliable. TRN [1] leverages onboard sensors, primarily cameras and inertial measurement units, to detect and track natural terrain features like craters, rocks, and slopes, providing accurate localization in real time. TRN is critical for precise lunar operations, including safe landings near scientifically or operationally valuable sites, autonomous rover traversal over hazardous terrain, and extended missions in regions with limited communication or lighting. It underpins advanced exploration objectives, in-situ resource utilization, and sustained robotic or human presence on the Moon.

In this work, we present a simulation and control framework for a lunar rover operating in low-gravity environments. To address the challenges of real-time localization and traversal on the Moon, this work makes the following contributions:

- **High-Fidelity Lunar Simulation:** We developed a dynamic model of a six-wheeled Rocker-Bogie rover within the MuJoCo physics engine, configured with a lunar gravity environment ($g = -1.62m/s^2$) to analyze suspension behavior and wheel-terrain interactions realistic to lunar missions.
- **EKF-Based Sensor Fusion:** We implemented an Extended Kalman Filter (EKF) to enable real-time state estimation. By fusing linear velocity data from wheel encoders with angular velocity from the Inertial Measurement Unit (IMU), this approach addresses the computational latency of visual odometry and corrects for wheel slip inherent in loose terrain.
- **Stability-Aware Navigation:** We designed a control architecture that integrates the EKF state estimates with a stability monitoring system, enabling the rover to autonomously navigate waypoints while actively mitigating tip-over risks on uneven terrain.

II. Related Work

Terrain Relative Navigation (TRN) is a localization technique in which a spacecraft or rover estimates its position and orientation by comparing real-time sensor observations (e.g, typically images, lidar, or other terrain measurements) to features of the surrounding landscape. Because the Moon lacks GPS, TRN provides a critical means of achieving accurate, autonomous navigation, precision landing, and hazard avoidance by leveraging the geometric structure of the terrain itself.

TRN research generally follows two major paradigms: map-based and mapless approaches. Map-based methods rely on pre-constructed terrain models to support global localization and hazard assessment. [2] creates high-resolution lunar surface maps by integrating orbital and surface datasets, providing reliable geometric references for TRN pipelines. Extending this paradigm, ShadowNav [3] performs localization in permanently shadowed regions by aligning non-visual sensor cues to prior maps when imagery is unavailable, demonstrating the robustness of map-dependent TRN even in extreme lighting conditions. In contrast, mapless TRN avoids reliance on stored terrain models and instead extracts navigation cues directly from live imagery. [4] shows that pose estimation can be achieved from monocular images using feature tracking and geometric constraints alone. Similarly, LunarNav [5] uses CNN-based crater detection to identify natural landmarks and localize without referencing a global map. Together, these works highlight complementary strategies for achieving reliable lunar navigation across both mapped and unmapped environments.

Moreover, previous planetary missions, such as Preseverrance Mars Rover [6], largely relied on manual ground-in-the-loop interventions for navigation and positioning. Operators on Earth analyzed images and telemetry data to plan rover paths, which limited responsiveness and autonomy, especially in dynamic or time-sensitive scenarios.

Our work aligns with mapless TRN approaches, which solve the navigation problem using only onboard sensor measurements. By leveraging camera-based observations and performing Visual-Inertial Odometry (VIO), our system enables the rover to localize autonomously, navigate effectively, and avoid hazardous terrain without relying on any pre-built lunar maps.

III. Method

A. Rockie-Bogie Rover

The Rocker-Bogie Rover is simulated in MuJoCo as a six-wheeled vehicle designed for low-gravity environments, such as the Moon, with gravity set to $-1.62\ \mathrm{m/s^2}$. Its suspension system combines bogie and rocker mechanisms, allowing the rover to maintain stability while traversing uneven terrain. Each wheel is equipped with a rotational joint and controlled by motor actuators, enabling precise speed control and torque feedback. The rover is equipped with an IMU and gyro sensors

to capture orientation and angular velocity, while a forward-mounted stereo camera mast provides visual perception. The ground is modeled as a large frictional plane, and collision, damping, and inertia parameters are tuned to produce realistic interactions between the wheels and terrain. Table I shows details about the Rockie-Bogie Rover simulated in MuJoCo.

TABLE I
MAIN COMPONENTS OF THE ROCKER-BOGIE ROVER

No.	Component	Dimensions / FOV	Weight (kg)
1	Chassis (Root Body)	0.15 × 0.125 × 0.025 m	8.0
2	Left Bogie Front Wheel	Cylinder: 0.0575 × 0.0375 m	0.3
3	Left Bogie Rear Wheel	Cylinder: 0.0575 × 0.0375 m	0.3
4	Left Rocker Rear Wheel	Cylinder: 0.0575 × 0.0375 m	0.3
5	Right Bogie Front Wheel	Cylinder: 0.0575 × 0.0375 m	0.3
6	Right Bogie Rear Wheel	Cylinder: 0.0575 × 0.0375 m	0.3
7	Right Rocker Rear Wheel	Cylinder: 0.0575 × 0.0375 m	0.3
8	Camera Mast	Cylinder: 0.02 × 0.15 m	0.05
9	Left Camera	FOV: 30°	0.01
10	Right Camera	FOV: 30°	0.01

B. Concept of Operations of Mission

The primary objective of the rover is to autonomously traverse a set of pre-defined waypoints $W = \{w_1, w_2, \ldots, w_N\}$ in a simulated lunar environment. The mission profile requires the rover to navigate complex trajectories, including straight sprints, S-curves, and circular surveys, to validate the stability and estimation frameworks.

Specific mission operation The autonomous operation cycle functions at a control frequency of 1 kHz. At each time step k, the rover performs the following operations:

1) State Estimation: The rover predicts its global pose $\mathbf{x}_k = [x_k, y_k, \theta_k]^T$ using an Extended Kalman Filter (EKF). The state propagation is governed by the discrete-time unicycle motion model:

$$\begin{bmatrix} x_{k+1} \\ y_{k+1} \\ \theta_{k+1} \end{bmatrix} = \begin{bmatrix} x_k + v_k \cos(\theta_k)\Delta t \\ y_k + v_k \sin(\theta_k)\Delta t \\ \theta_k + \omega_k \Delta t \end{bmatrix} + \mathbf{w}_k \tag{1}$$

where v_k is the linear velocity derived from wheel encoders, ω_k is the angular velocity from the IMU gyroscope, and $\mathbf{w}_k \sim \mathcal{N}(0, Q)$ represents process noise. IMU measurements are combined with Lucas–Kanade optical flow tracking to predict the rover's global pose

2) Path Planning and Control: The path planner computes the heading error θ_{err} relative to the current target waypoint w_i. A proportional controller drives the angular velocity to minimize this error. The resulting target velocities (v_{cmd}, ω_{cmd}) are converted into individual wheel velocities $\omega_{L,R}$ using differential drive kinematics:

$$\omega_{L,R} = \frac{v_{cmd} \mp (\omega_{cmd} \cdot \frac{L}{2})}{r} \tag{2}$$

where L is the track width (0.4 m) and r is the wheel radius (0.05 m). This control loop continues until the Euclidean distance to the waypoint falls below the tolerance threshold δ.

C. Dynamic Modeling of the Rocker-Bogie Rover

The rover is simulated as a six-wheeled articulated system in MuJoCo, where the chassis is a free-floating body connected to wheels via revolute joints along their axles. The rockers and bogies form the passive suspension, allowing the chassis to adapt to uneven terrain. The dynamics are governed by

$$\mathbf{M}(\mathbf{q})\ddot{\mathbf{q}} + \mathbf{C}(\mathbf{q}, \dot{\mathbf{q}})\dot{\mathbf{q}} + \mathbf{G}(\mathbf{q}) = \tau + \mathbf{J}^\top \mathbf{F}_{\text{contact}},$$

where:

- $\mathbf{q}$ and $\dot{\mathbf{q}}$ are the generalized positions and velocities of the rover.
- $\mathbf{M}(\mathbf{q})$ is the mass/inertia matrix of the system.
- $\mathbf{C}(\mathbf{q}, \dot{\mathbf{q}})$ represents Coriolis and centrifugal effects.
- $\mathbf{G}(\mathbf{q})$ is the gravitational force vector.
- τ is the vector of wheel actuator torques applied by the controller.
- $\mathbf{J}^\top \mathbf{F}_{\text{contact}}$ accounts for forces from wheel-terrain contacts.

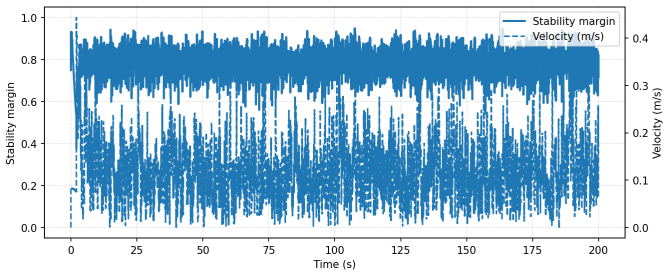

Fig. 1. Method Performance

D. Analysis

The telemetry data from the autonomous exploration mission is presented in Figure 1.

Stability Performance: The stability margin remained consistently robust, oscillating between 0.6 and 0.9. This confirms that the Rocker-Bogie suspension effectively minimizes chassis pitch and roll in lunar gravity ($g = -1.62 m/s^2$), keeping the rover well above the critical tip-over threshold of 0.3.

Velocity and Linearity: The velocity profile exhibits high-frequency non-linear oscillations, fluctuating rapidly between 0.0 and 0.4 m/s. This behavior suggests significant wheel slip or aggressive PID gains ($K_p = 20.0$), resulting in a "stop-and-go" motion rather than a linear steady-state cruise.

IV. RESULTS

A. Experimental Setup

The experimental trials were conducted in the MuJoCo physics engine with a simulation duration of $t = 200$ seconds. The environment was configured with lunar gravity ($g = -1.62 m/s^2$) and a high-friction coefficient terrain model to simulate regolith interactions. The rover was tasked with autonomously navigating a $12m \times 12m$ grid of waypoints using the EKF-based control loop described in Section III.

B. Stability and Traversal

As shown in the mission summary (Fig. 1), the Rocker-Bogie suspension demonstrated excellent passive stability. The stability margin remained consistently high, oscillating between 0.6 and 0.9, well above the critical tip-over threshold.

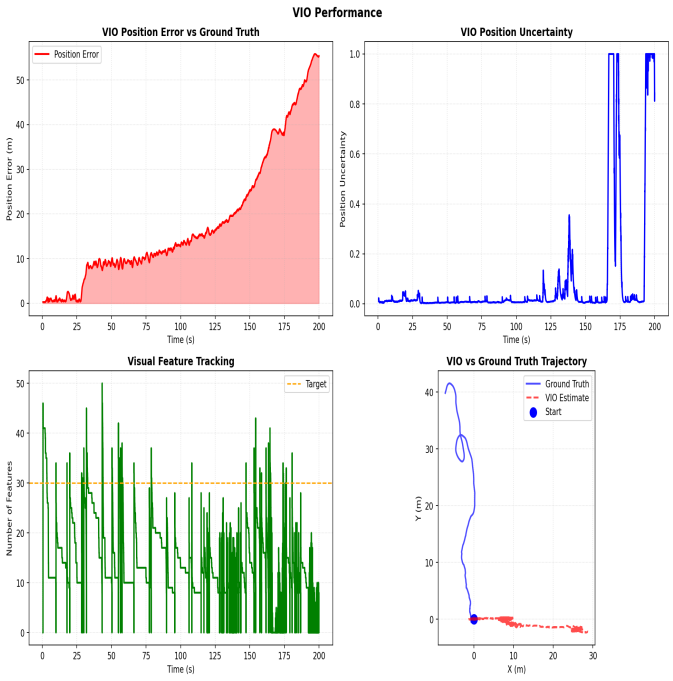

Fig. 2. Method Performance: The divergence between the VIO/EKF estimate (Red) and Ground Truth (Blue) highlights the impact of wheel slip on odometry-based estimation.

C. Estimation Performance and Validation

The estimation analysis (Fig. 2) validates the realistic modeling of lunar surface challenges.

- **Position Error Drift:** The position error accumulates monotonically, reaching approximately $55m$ by $t = 200s$.
- **Trajectory Divergence:** The "VIO vs Ground Truth" plot reveals a critical divergence. The red dashed line (Estimate) shows the rover "thinking" it is traveling roughly 30 meters along the X-axis. Conversely, the blue line (Ground Truth) shows the rover actually drifting along the Y-axis while remaining near the origin.

This discrepancy validates the simulation's fidelity regarding wheel slip. The EKF relies on wheel odometry; because the wheels were spinning (generating encoder counts) but not gripping the terrain, the estimator predicted forward motion while the physical rover remained stationary or slip laterally. This confirms that odometry-based estimation alone is insufficient for low-gravity, loose-terrain environments. Also, the positon error could also be due to the fact that there are few distinctive features over the lunar surface and it is hard to track features over time due.

V. Conclusion

In this project, we successfully developed and simulated a six-wheeled Rocker-Bogie rover within a high-fidelity MuJoCo lunar environment. The simulation effectively captured the complex dynamics of low-gravity exploration, including suspension compliance and wheel-terrain interactions. We implemented an Extended Kalman Filter (EKF) to fuse wheel odometry with IMU gyro data, replacing computationally expensive visual odometry with a real-time sensor fusion framework. The experimental results validated the passive stability of the Rocker-Bogie mechanism, which maintained a safety margin above 0.6 even under aggressive maneuvering. However, the results also highlighted a critical limitation in odometry-based navigation on the Moon: wheel slip. Due to the low-gravity environment ($g = -1.62m/s^2$), the rover experienced significant traction loss, causing the EKF to overestimate the traveled distance by approximately 55 meters over a 200-second mission. This divergence confirms that while kinematic models are sufficient for stability, they are insufficient for accurate localization in loose regolith.

To improve upon these results and address the localization drift caused by wheel slip, future developments should focus on two key areas:

- **Visual-Inertial Odometry (VIO):** To correct for wheel slip, the system requires exteroceptive sensing. Re-integrating a hardware-accelerated Visual Odometry pipeline would allow the rover to track static terrain features, providing a ground-truth correction signal to the EKF when wheels spin without traction. Since textureless lunar regolith offers few stable keypoints, introducing distinctive terrain elements such as craters can greatly enhance feature detection and tracking, thereby improving the robustness and accuracy of VIO.
- **Traction Control:** Implementing an active traction control system that monitors the discrepancy between the commanded wheel velocity and the IMU acceleration could minimize slip before it occurs, improving the reliability of the wheel odometry data.

References

[1] A. I. Mourikis et al., "Vision-aided inertial navigation for spacecraft entry, descent, and landing," *IEEE Transactions on Robotics*, vol. 25, no. 2, pp. 264–280, 2009. DOI: 10.1109/TRO.2009.2012342.

[2] C. I. Restrepo et al., "Building lunar maps for terrain relative navigation and hazard detection applications," in *AIAA SCITECH 2022 Forum*. DOI: 10.2514/6.2022-0356. eprint: https://arc.aiaa.org/doi/pdf/10.2514/6.2022-0356. [Online]. Available: https://arc.aiaa.org/doi/abs/10.2514/6.2022-0356.

[3] D. Atha et al., "Shadownav: Autonomous global localization for lunar navigation in darkness," *IEEE Transactions on Field Robotics*, 2024.

[4] J. A. Christian et al., "Image-based lunar terrain relative navigation without a map: Measurements," *Journal of Spacecraft and Rockets*, vol. 58, no. 1, pp. 164–181, 2021. DOI: 10.2514/1.A34875. eprint: https://doi.org/10.2514/1.A34875. [Online]. Available: https://doi.org/10.2514/1.A34875.

[5] L. M. Downes, T. J. Steiner, and J. P. How, "Lunar terrain relative navigation using a convolutional neural network for visual crater detection," in *2020 American Control Conference (ACC)*, IEEE, 2020, pp. 4448–4453.

[6] V. Verma et al., “Autonomous robotics is driving perseverance rover’s progress on mars,” *Science Robotics*, vol. 8, no. 80, eadi3099, 2023. DOI: 10.1126/scirobotics.adi3099. eprint: https://www.science.org/doi/pdf/10.1126/scirobotics.adi3099. [Online]. Available: https://www.science.org/doi/abs/10.1126/scirobotics.adi3099.